

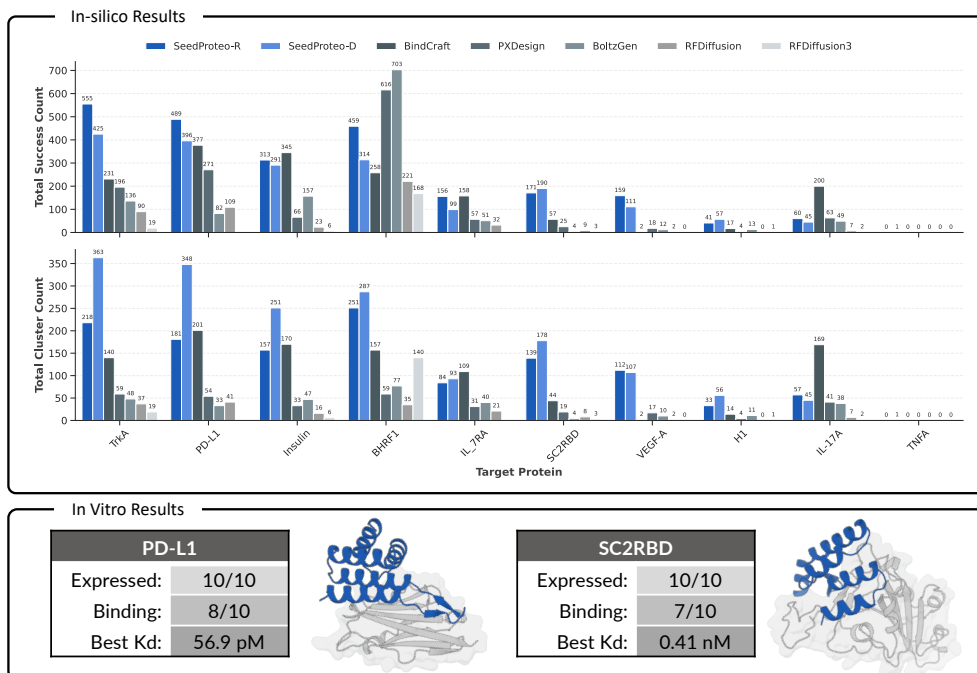
# SeedProteo: Accurate De Novo All-Atom Design of Protein Binders

<sup>1</sup>ByteDance Seed

Full author list in Contributions

## Abstract

We present SeedProteo, a diffusion-based model for *de novo* all-atom protein design. We demonstrate how to repurpose a cutting-edge folding architecture into a powerful generative design framework by effectively integrating self-conditioning features. Extensive benchmarks highlight the model’s capabilities across two distinct tasks: in unconditional generation, SeedProteo exhibits superior length generalization and structural diversity, maintaining robustness for long sequences and complex topologies; in binder design, it achieves state-of-the-art performance among open-source methods, attaining the highest in-silico design success rates, structural diversity and novelty. Finally, we validate SeedProteo through wet-lab assays on two therapeutic targets, achieving hit rates of 70%–80% and picomolar-level binding affinities, establishing leading results. To facilitate community adoption, we provide public access to SeedProteo via a webserver (<https://seedfold.io/proteinDesign>).



Date: Feb 24, 2026

Correspondence: Quanquan Gu ([quanquan.gu@bytedance.com](mailto:quanquan.gu@bytedance.com))

Project Page: <https://seedfold.github.io/>

# 1 Introduction

Proteins perform a vast array of functions within organisms. As the evolution process spans millions to billions of years, the field of protein design aims to automate and accelerate it through computational methods. Since the function of proteins is conferred via the structure, which is determined by the sequence, a line of research focuses on generating sequences [1–4] and structures [5–8]. Recently, a new paradigm has emerged emphasizing the co-generation of sequence and structure [9–12]. However, improving sample diversity while preserving the coherence between modalities, specifically sequence-structure consistency, remains a formidable challenge. To address this, recent works have pivoted toward all-atom modeling [13, 14]. By directly designing proteins at the all-atom level, these methods naturally derive amino acid identities from atomic coordinates, achieving superior consistency. These methodological advancements have significantly propelled the field of *de novo* protein design, particularly in binder design, the creation of mini-binders for specific therapeutic targets [15]. This domain has witnessed a rapid evolution, progressing from classical hallucination-based methods [16] or backbone-based design model [8, 17] to the current wave of all-atom diffusion models [18–20], all striving for enhanced designability and binding affinity.

In this study, we introduce **SeedProteo**, a diffusion-based model that learns the manifold of proteins at the all-atom level. SeedProteo mimics the architecture of AlphaFold3 [21–23], which has proven its effectiveness in protein folding. Through unifying the representation of different amino acids, we significantly enhance its generative power when the protein sequence and homology are not provided. A major issue in all-atom modeling is the backbone-sidechain inconsistency (i.e., the sequence-structure inconsistency), which means that the sidechain atoms are locally plausible but the derived sequence fails to fold into the global backbone structure. SeedProteo iteratively evolves the sequence and structure and integrates two components to enhance the modeling ability of two modalities: (i) SeedProteo enhances the structural feasibility through the integration of geometric reasoning in the denoising process. To be specific, we reuse the denoised structure from the previous timestep [24] to stabilize the sampling process and conduct geometric reasoning in the pair representation space. (ii) SeedProteo conducts energy minimization within the sequence space modeled by a Markov random field (MRF) [25]. By integrating high-order couplings among distinct positions, we are able to sample globally feasible sequences and prevent being trapped in the local minima of simple patterns constituted by high-frequency amino acids. We conduct extensive experiments on unconditional sampling, binder design, and in vitro validation. The results demonstrate that:

- 1) In unconditional generation, SeedProteo exhibits superior length generalization and structural diversity compared to state-of-the-art baselines. It maintains stable performance on long sequences (up to 1000 residues) and complex topologies, effectively addressing the length-dependent degradation issues observed in baseline diffusion models.
- 2) In binder design, to address the trade-off between design success rate and structural diversity, we introduce two inference modes: **SeedProteo-R** (Robust), which prioritizes longer secondary structure segments for higher design success, and **SeedProteo-D** (Diverse), which fosters topological richness. Experiments show robust performance across diverse targets, particularly excelling in challenging cases.
- 3) Furthermore, our analysis offers specific insights into how to achieve superior sequence-structure consistency within the `atom14` representation schema [13, 18, 26]. We demonstrate that introducing a global MRF-based decoding module leads to more self-consistent outputs.
- 4) Beyond in-silico evaluation, we further validate SeedProteo with wet-lab experiments, demonstrating that designed binders exhibit strong binding in SPR assays with high hit rates across multiple therapeutic targets.

## 2 Method

### 2.1 Model Architecture

SeedProteo is a diffusion-based all-atom protein generation model specifically designed for binder design. To enable direct modeling of all-atom structures, the primary challenge lies in representing side-chain atoms when amino acid types are unknown. To address this issue, SeedProteo introduces virtual atoms and adopts

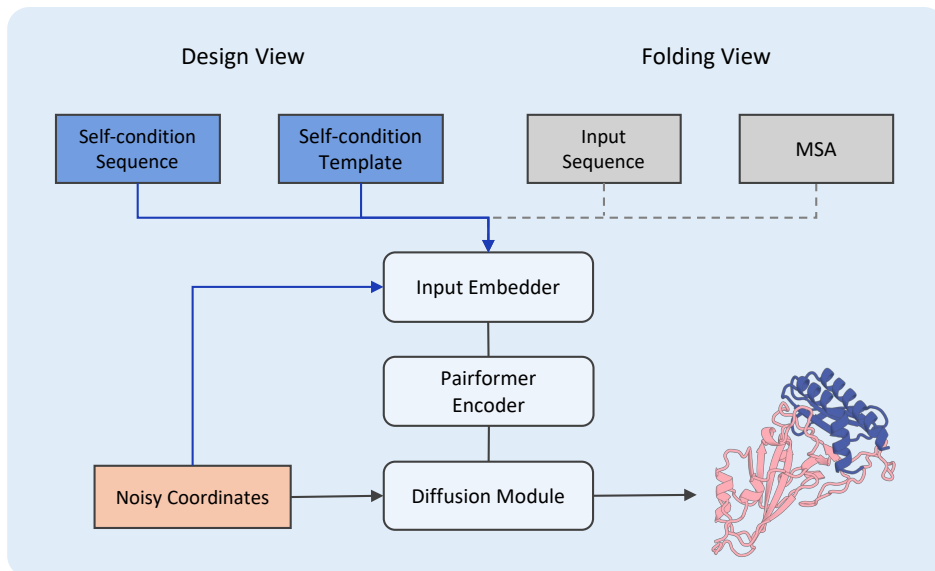


**Figure 1** Overview of the SeedProteo framework. The right panel illustrates the input representation from a folding perspective. By modifying specific input channels within a nearly identical network architecture, we adapt the framework into the generative design model shown on the left.

the `atom14` schema [13] for all amino acids, which includes four backbone atoms and ten side-chain atoms, with virtual atoms overlaid on the  $C\alpha$  atom.

As shown in Figure 1, SeedProteo leverages the powerful non-equivariant atomic coordinate modeling capability of AF3-like folding model architectures, and therefore adopts a network structure consistent with such folding models: (i) an embedder module for feature initialization, (ii) an encoder composed of Pairformer blocks, and (iii) a diffusion module that denoises coordinates based on the encoder’s representations.

However, a key challenge arises because the folding model’s encoder is sequence-based. A trivial solution would be to replace the sequence with all [MASK] tokens, but such a degenerate biased input would render the encoder ineffective. To address this issue, SeedProteo additionally feeds noisy coordinates into the encoder to extract intrinsic geometric relationships: within the embedder, noisy coordinates are transformed into 1D sequence representation. This modification, however, introduces a computational cost—since the encoder, which contains cubic algorithmic complexity, becomes dependent on the noisy inputs. To mitigate the computational burden, we reduced the number of Pairformer layers from 48 to 12.

## 2.2 Self-conditioning features

The distribution of protein atomic coordinates constitutes a specialized manifold. Although diffusion models can directly learn this coordinate distribution, a simple diffusion process lacking constraints often leads to the generation of structures that are geometrically plausible yet physically unrealizable. These generated backbones often exhibit poor designability, meaning that no amino acid sequence can stably fold into the generated conformation. Consequently, sequences derived from inverse folding on these structures typically fail to adopt the intended topology. Recent advances in protein design methodologies have validated the effectiveness of self-conditioning. We posit that employing effective self-conditioning features represents a promising pathway for substantially enhancing design capabilities. The following features are utilized as conditioning inputs in our model.

1. **Sequence Sampling:** SeedProteo employs a Markov Random Field (MRF)-based Sequence Module [27, 28] to decode amino acid sequences. The probability of a sequence  $\mathbf{x}$  is parameterized using the

learned pair and single representations (Eq. 1):

$$P(\mathbf{X} = \mathbf{x} \mid \mathbf{a}, \mathbf{z}) \propto \exp \left[ \sum_{i=1}^L h_i(x_i \mid \mathbf{a}_i) + \sum_{i=1}^L \sum_{j=i+1}^L e_{ij}(x_i, x_j \mid \mathbf{z}_{ij}) \right], \quad (1)$$

where  $\mathbf{x} = (x_1, \dots, x_L)$  denotes the target amino acid sequence of length  $L$ , and  $\mathbf{a}, \mathbf{z}$  represent the learned single and pair representations, respectively. The term  $h_i(\cdot)$  models the site-specific bias for amino acid  $x_i$  conditioned on the single feature  $\mathbf{a}_i$ , while  $e_{ij}(\cdot)$  captures the pairwise coupling propensity between residues  $x_i$  and  $x_j$  derived from the pair feature  $\mathbf{z}_{ij}$  [29]. We observe that this sequence-guided approach enhances the model’s co-design capability by mitigating potential conflicts between sequence and structural constraints. By integrating the MRF module, SeedProteo eliminates the need to infer amino acid types by translating `atom14` coordinates. Instead, it directly utilizes the sequence inferred by the MRF, which incorporates semantic information to avoid misclassification of structurally similar (isosteric) amino acids, as the final output sequence.

2. **Secondary Structure Sequence:** SeedProteo accepts a secondary structure (SS) sequence [30] composed of three canonical characters (H, E, L) and a special mask token (X). The model performs unmasking predictions based on the input masked SS sequence and subsequently utilizes the predicted SS sequence for self-conditioning (Eq. 2):

$$\begin{aligned} \mathcal{S}^{(0)} &= \mathcal{S}_{\text{input}} \\ \mathcal{S}_{\text{pred}}^{(t)} &= f_{\theta} \left( \mathcal{S}_{\text{cond}}^{(t-1)} \right) \\ \mathcal{S}_{\text{cond}}^{(t)} &= \alpha_t \cdot \mathcal{S}_{\text{pred}}^{(t)} + (1 - \alpha_t) \cdot \mathcal{S}_{\text{cond}}^{(t-1)}, \end{aligned} \quad (2)$$

where  $\mathcal{S}_{\text{input}}$  represents the initial, potentially masked secondary structure representation. At iteration  $t$ ,  $f_{\theta}(\cdot)$  denotes the neural network predictor parameterized by  $\theta$ , yielding the unmasked prediction  $\mathcal{S}_{\text{pred}}^{(t)}$ . This prediction is integrated into the conditioning state  $\mathcal{S}_{\text{cond}}^{(t)}$  via a scalar gating factor  $\alpha_t \in [0, 1]$ , which controls the update rate of the self-conditioning signal. This capability enables SeedProteo to process arbitrarily generated SS sequences, even those containing unknown segments, and adaptively refine them into a physically plausible SS sequence. We demonstrate that incorporating secondary structure features effectively guides the generation of *de novo*-like structures, significantly enhancing the success rate in binder design applications.

3. **Structural Template:** SeedProteo utilizes the denoised structure obtained from the previous step as a structural template for self-conditioning. Specifically, a binning operation is applied to convert the  $C_{\beta}$  distance map into a one-hot tensor, which serves as a pairwise feature. We demonstrate that incorporating such template features helps stabilize the structural sampling trajectory.

### 2.3 Training Objective

SeedProteo employs a set of loss functions commonly used in AF3-like folding models [21], including a coordinate diffusion loss, a smooth LDDT loss, and a distogram loss. The coordinate diffusion loss is applied without pre-aligning the target and predicted structures, thereby compelling the model to learn equivariance directly through this loss. Additionally, a cross-entropy loss is used to supervise the MRF-sampled sequence and the predicted secondary structure sequence.

### 2.4 Training Pipeline

SeedProteo was trained from scratch. Inspired by the training strategies of folding models, we adopted a multi-stage training pipeline. In the first stage, the model was trained using a small crop size and strictly filtered monomer data. In the second stage, training continued with a larger crop size and an expanded dataset comprising comprehensively filtered monomer data. Meanwhile, motifs are incorporated during the training process with monomer data, where partial structures paired with corresponding sequences are provided to enhance the model’s responsiveness to conditional inputs. In the third stage, the large crop size

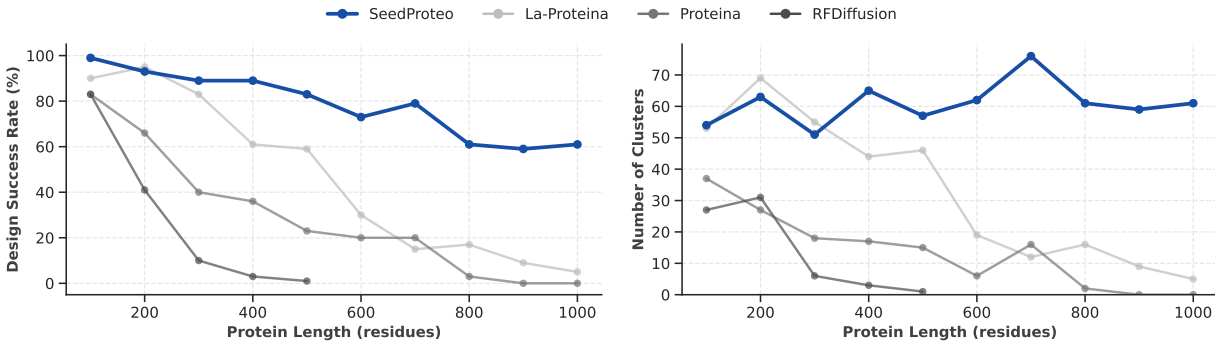


**Figure 2** Unconditional monomer benchmark. Stricter thresholds are applied to define designability (in Appendix B).

was maintained, and training proceeded with a balanced 1:1 sampling ratio of monomer data and protein multimer data. Detailed descriptions of the datasets and hyperparameters are provided in (Appendix A and Table 5).

### 3 In-silico Results

We evaluated SeedProteo on two primary tasks: unconditional protein monomer generation and protein binder design. Unconditional generation refers to designing monomeric proteins starting from Gaussian noise, which serves to assess the model’s fundamental generative capability. Binder design, on the other hand, involves generating potential high-affinity binders based on the full atomic information of a given target protein, with the goal of enabling real-world applications.

Although numerous diffusion-based co-design methods are capable of jointly generating sequences and structures (in either backbone or all-atom form), existing results consistently indicate that the sequence consistency of their outputs is generally lower than that achieved by redesigning structures using ProteinMPNN [1]. Therefore, in the subsequent evaluations, for the structures generated by diffusion-based methods, we employed ProteinMPNN for sequence redesign to ensure fair and comparable assessments. Regarding the details of the evaluation procedure and the definitions of the metrics, please refer to Appendix B.

#### 3.1 Unconditional Generation Benchmark

##### 3.1.1 Scalability and Structural Diversity

We first evaluate SeedProteo against state-of-the-art diffusion-based baselines, La-Proteina [14], Proteina [31], and RFDiffusion [6], on the task of unconditional monomer generation. We focus on two critical dimensions: *scalability* to long sequences and *structural diversity*. As illustrated in Figure 2 (Left), SeedProteo consistently achieves superior design success rates across the entire length spectrum (100–1000 residues). While competing methods exhibit a sharp performance degradation as sequence length increases, dropping to near-zero success rates beyond 600 residues, SeedProteo maintains robust performance, achieving a success rate of > 60% even at length 1000. This suggests that our method effectively models the long-range dependencies and global constraints inherent in large protein assemblies, a capability that current baselines lack. In addition to quality, SeedProteo excels in generative diversity. Figure 2 (Right) plots the number of unique structural clusters found within the successful samples. Notably, as protein length increases, baselines suffer from severe mode collapse (e.g., RFDiffusion and Proteina generate few to no unique clusters at long lengths). In contrast, SeedProteo sustains a high volume of unique clusters, indicating that it captures a richer and more generalizable distribution of the protein structure space.

##### 3.1.2 Fine-grained Evaluation across Structural Topologies

Previous generative models often exhibit a strong preference for simple  $\alpha$ -helical architectures [6, 13], frequently failing to generalize to complex topologies such as all- $\beta$  sheets. Our empirical observations confirm that

**Table 1 Unconditional Design Benchmark Performance across Structural Topologies.** We compare **SeedProteo** against baselines on three different fold types:  $\alpha$ -helix bundles (HHH), Hybrid (HEL), and  $\beta$ -sheets (EEE). Metrics reported in order: Design Success Rate (**Succ.**,  $\uparrow$ ), Unique Success Clusters (**Uniq.**,  $\uparrow$ ), and Novelty (**Nov.**,  $\downarrow$ ). The best performance is highlighted in **bold**. Dash (–) indicates model failure or insufficient successful samples.

Panel A: Primarily $\alpha$ -Helix (HHH) Structures												
Length	SeedProteo (Ours)			La-Proteina			Proteina			RFDiffusion		
	Succ. $\uparrow$	Uniq. $\uparrow$	Nov. $\downarrow$	Succ. $\uparrow$	Uniq. $\uparrow$	Nov. $\downarrow$	Succ. $\uparrow$	Uniq. $\uparrow$	Nov. $\downarrow$	Succ. $\uparrow$	Uniq. $\uparrow$	Nov. $\downarrow$
100	<b>100%</b>	17	0.89	93%	<b>27</b>	0.86	88%	22	<b>0.83</b>	87%	19	0.89
200	<b>96%</b>	24	0.85	<b>96%</b>	<b>60</b>	<b>0.80</b>	73%	21	0.83	73%	8	0.85
300	<b>95%</b>	24	0.83	85%	<b>47</b>	<b>0.80</b>	51%	13	0.88	–	–	–
400	<b>98%</b>	32	0.79	61%	<b>40</b>	<b>0.76</b>	39%	14	0.88	–	–	–
500	<b>90%</b>	36	0.81	67%	<b>43</b>	<b>0.74</b>	33%	12	0.85	–	–	–
600	<b>86%</b>	<b>38</b>	<b>0.79</b>	43%	9	0.88	27%	6	0.89	–	–	–
700	<b>86%</b>	<b>49</b>	<b>0.82</b>	38%	6	0.83	24%	15	0.89	–	–	–
800	<b>65%</b>	<b>39</b>	<b>0.79</b>	41%	10	0.86	4%	2	0.96	–	–	–
900	<b>66%</b>	<b>45</b>	<b>0.75</b>	41%	7	0.88	–	–	–	–	–	–
1000	<b>63%</b>	<b>41</b>	<b>0.77</b>	31%	5	0.88	–	–	–	–	–	–

Panel B: Hybrid Helix-E-Loop (HEL) Structures												
Length	SeedProteo (Ours)			La-Proteina			Proteina			RFDiffusion		
	Succ. $\uparrow$	Uniq. $\uparrow$	Nov. $\downarrow$	Succ. $\uparrow$	Uniq. $\uparrow$	Nov. $\downarrow$	Succ. $\uparrow$	Uniq. $\uparrow$	Nov. $\downarrow$	Succ. $\uparrow$	Uniq. $\uparrow$	Nov. $\downarrow$
100	<b>97%</b>	26	<b>0.82</b>	87%	<b>27</b>	0.86	87%	13	<b>0.82</b>	71%	12	0.85
200	<b>92%</b>	<b>32</b>	<b>0.79</b>	90%	7	0.81	55%	6	0.82	38%	22	0.80
300	<b>81%</b>	<b>21</b>	<b>0.77</b>	72%	8	0.83	15%	4	0.85	11%	6	0.78
400	<b>79%</b>	<b>26</b>	<b>0.77</b>	62%	3	0.79	12%	2	0.91	3%	3	0.80
500	<b>69%</b>	<b>20</b>	<b>0.75</b>	60%	3	0.83	5%	2	0.87	1%	1	0.76
600	<b>57%</b>	<b>23</b>	<b>0.77</b>	26%	12	0.85	–	–	–	–	–	–
700	<b>72%</b>	<b>28</b>	<b>0.77</b>	9%	6	0.88	9%	1	0.93	–	–	–
800	<b>56%</b>	<b>22</b>	<b>0.79</b>	11%	6	0.86	–	–	–	–	–	–
900	<b>44%</b>	<b>14</b>	<b>0.78</b>	3%	2	0.89	–	–	–	–	–	–
1000	<b>57%</b>	<b>20</b>	<b>0.74</b>	–	–	–	–	–	–	–	–	–

Panel C: Primarily $\beta$ -Sheet (EEE) Structures												
Length	SeedProteo (Ours)			La-Proteina			Proteina			RFDiffusion		
	Succ. $\uparrow$	Uniq. $\uparrow$	Nov. $\downarrow$	Succ. $\uparrow$	Uniq. $\uparrow$	Nov. $\downarrow$	Succ. $\uparrow$	Uniq. $\uparrow$	Nov. $\downarrow$	Succ. $\uparrow$	Uniq. $\uparrow$	Nov. $\downarrow$
100	<b>100%</b>	<b>12</b>	<b>0.80</b>	<b>100%</b>	1	0.88	50%	3	0.84	–	–	–
200	86%	<b>6</b>	<b>0.80</b>	<b>100%</b>	2	0.84	–	–	–	20%	1	0.75
300	<b>80%</b>	<b>4</b>	<b>0.80</b>	–	–	–	25%	1	0.85	–	–	–
400	<b>73%</b>	<b>7</b>	<b>0.80</b>	50%	1	0.85	57%	2	0.85	–	–	–
500	<b>50%</b>	<b>1</b>	<b>0.68</b>	–	–	–	50%	1	0.74	–	–	–
600	–	–	–	<b>25%</b>	<b>4</b>	<b>0.86</b>	–	–	–	–	–	–
700	–	–	–	<b>8%</b>	<b>1</b>	<b>0.86</b>	–	–	–	–	–	–

Note: Only lengths up to 700 are shown for EEE as all methods failed to generate valid long  $\beta$ -sheet structures.

**Table 2 Structural Novelty ( $\downarrow$ ) in Binder Design Benchmark.** Transposed comparison of average novelty scores. We compare **SeedProteo** variants against baselines across ten targets. **Lower is Better**. Best performance per target is highlighted in **bold**, and the second best is underlined.

Method	TrkA	PD-L1	Insulin	BHRF1	IL-7RA	SC2RBD	VEGF-A	H1	IL-17A	TNFA
<b>Ours</b>										
SeedProteo-D	<u>0.829</u>	<b>0.832</b>	<b>0.837</b>	<b>0.822</b>	<b>0.840</b>	<b>0.819</b>	<b>0.836</b>	<b>0.823</b>	<u>0.806</u>	<b>0.870</b>
SeedProteo-R	0.905	0.913	0.911	0.872	0.917	<u>0.858</u>	0.901	0.890	0.855	-
<b>Baselines</b>										
BindCraft	0.849	0.856	<u>0.864</u>	0.847	<u>0.861</u>	0.863	<u>0.850</u>	<u>0.830</u>	0.818	-
PXDesign	0.914	0.929	0.928	0.924	0.928	0.917	0.913	0.888	0.906	-
BoltzGen	0.908	0.924	0.929	0.928	0.885	0.915	0.902	0.885	0.863	-
RFDiffusion	0.932	0.934	0.927	0.946	0.916	0.912	0.940	-	0.938	-
RFDiffusion3	<b>0.808</b>	<u>0.834</u>	0.876	<u>0.845</u>	<b>0.840</b>	-	-	0.930	<b>0.800</b>	-

designability is highly topology-dependent: primarily  $\beta$ -sheet structures consistently yield lower success rates compared to helical bundles across all models. To dissect this phenomenon, we present a fine-grained evaluation in Table 1, breaking down performance by three distinct topologies: primarily  $\alpha$ -helix (HHH), primarily  $\beta$ -sheet (EEE) and hybrid Helix-Sheet-Loop (HEL). The results reveal a distinct advantage for SeedProteo in handling complex folds:

- **Complex Topology Robustness:** In the Hybrid (HEL) category, SeedProteo achieves a 57% success rate at length 1000, whereas baselines largely fail to produce valid structures beyond length 600.
- **$\beta$ -Sheet Generation:** In the  $\beta$ -sheet (EEE) regime, which is notoriously difficult for generative models, SeedProteo is the only method capable of generating diverse, valid and novel structures (Success > 50% and Novelty < 0.8) at lengths up to 500. Other models suffer from complete generation failure or mode collapse in this category.
- **Novelty and Diversity:** Across all topologies, SeedProteo consistently achieves higher structural diversity (Unique Clusters) and favorable novelty scores, indicating that it does not merely retrieve training templates but effectively explores novel regions of the protein manifold.

### 3.2 Binder Design Benchmark

We benchmark SeedProteo against five leading open-source binder design methods: RFDiffusion [6], RFDiffusion3 [18], BoltzGen [26], PXDesign [17], and BindCraft [16]. Following the protocol established in AlphaProteo [15], we generate approximately 1,000 candidates for each of the 10 benchmark targets, uniformly covering the target-specific binder length ranges. For structure-generating diffusion models (SeedProteo, RFDiffusion variants, PXDesign, and BoltzGen), binder sequences are redesigned using ProteinMPNN. A notable exception is BindCraft, a hallucination-based approach [32], which optimizes sequences directly via gradient descent on folding metrics (e.g., ipTM). All designs are subsequently evaluated *in silico* using SeedFold [33]. We adopt the success criteria defined in AlphaProteo: minimum inter-chain Predicted Aligned Error (PAE)  $\leq 1.5$ , binder pTM  $\geq 0.8$ , and complex RMSD  $< 2.5\text{\AA}$ .

In SeedProteo, we introduce two distinct Secondary Structure (SS) sampling modes to balance the trade-off between designability and structural diversity:

- **SeedProteo-R:** This is a SS robust mode. Prioritizes fewer but longer continuous secondary structure segments. This mode imposes stronger structural stability constraints, typically yielding a higher design success number.
- **SeedProteo-D:** This is a SS diverse mode. Allows for a higher frequency of shorter secondary structure segments. This mode encourages more complex topologies, resulting in greater structural diversity at the cost of slightly reduced raw success number.

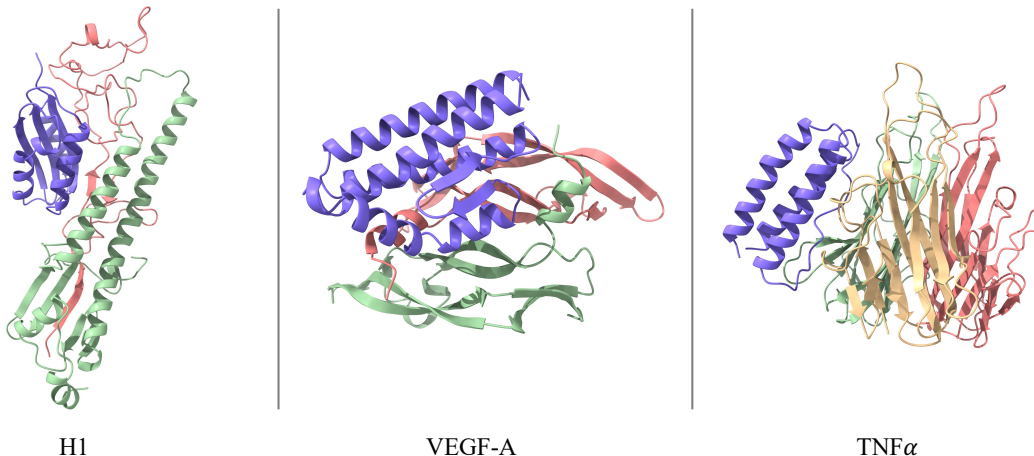


**Figure 3** Binders generated by SeedProteo for the challenging multi-chain targets H1 (dimer), VEGF-A (dimer), and TNF- $\alpha$  (trimer). All displayed binders, colored in purple, meet the in silico success criteria.

**Table 3** Benchmarking Co-design Capabilities of Diffusion-based Models for Binder Design.

Method	BHRF1	SC2RBD	IL-7RA	PD-L1	TrkA	Insulin	H1	VEGF-A	IL-17A	TNF $\alpha$
<i>Baselines</i>										
BoltzGen	<b>627</b>	0	10	17	21	99	1	1	5	0
RFDiffusion3	9	0	0	1	0	0	0	0	0	0
<i>SeedProteo (Ours)</i>										
SeedProteo-R	296	<b>92</b>	<b>100</b>	<b>380</b>	<b>232</b>	<b>303</b>	16	<b>127</b>	<b>47</b>	1
SeedProteo-D	139	80	52	265	143	181	<b>25</b>	45	17	<b>3</b>
SeedProteo-M	133	77	25	154	143	189	12	47	13	1

**Performance Analysis.** We evaluated the unconditional generation capabilities of SeedProteo across a diverse set of ten target proteins. As shown in Figure , SeedProteo-R demonstrates a commanding lead in total success counts across the benchmark. Notably, this advantage is most pronounced on challenging targets, specifically SC2RBD, VEGF-A, H1, and TNF $\alpha$ .

Beyond design success, structural diversity is a critical metric for downstream applicability. Figure highlights that SeedProteo-D excels in generating structurally distinct binders, achieving the highest number of unique success clusters in 8 out of the 10 targets. Complementing this structural diversity, Table 2 demonstrates that SeedProteo-D also achieves the best novelty scores for successfully designed binders in 8 out of the 10 targets. Notably, it consistently outperforms all baselines, except RFDiffusion3, across every target; for example, while baselines like PXDesign often yield scores above 0.9, SeedProteo-D maintains superior novelty with scores in the 0.8 range. This indicates that SeedProteo does not merely converge on a single solution but effectively explores the structural landscape to provide a diverse portfolio of high-quality and novel candidates. Figure 3 presents case studies on challenging targets.

### 3.3 Discussion on Co-Design Strategies

We here discuss the significance of co-design and methods for enhancing co-design capabilities. While two-stage pipelines (backbone generation followed by inverse folding) have dominated recent protein design benchmarks, our analysis suggests that simultaneous sequence-structure generation (co-design) offers potential advantages for complex targets.

**Table 4 Ablation Study on Sequence Decoding Strategies.**

Length	Decoding Method	scRMSD ↓	scTM ↑	pLDDT ↑	Succ. Rate ↑
100	Baseline (atom14)	<b>1.11</b>	<b>0.94</b>	88.56	<b>0.90</b>
	SeedProteo (MRF)	1.63	0.93	<b>88.65</b>	0.84
200	Baseline (atom14)	3.87	0.86	78.06	0.68
	SeedProteo (MRF)	<b>2.08</b>	<b>0.92</b>	<b>84.36</b>	<b>0.80</b>
300	Baseline (atom14)	4.71	0.83	73.40	0.52
	SeedProteo (MRF)	<b>2.30</b>	<b>0.91</b>	<b>80.33</b>	<b>0.76</b>

**Beyond the Inverse Folding Bottleneck** Empirical results (Figure and Table 3) indicate that, on average, sequences derived from ProteinMPNN achieve higher success rates than those generated via pure co-design. This is expected, as ProteinMPNN is highly optimized for fixed-backbone recovery. However, we argue that reliance on inverse folding alone is not the ultimate solution for *de novo* binder design.

A striking exception is observed with the TNF $\alpha$  target. Here, ProteinMPNN-based methods almost universally fail (0 or 1 success) shown in Figure , whereas our co-design approach yields valid binders. We reason that inverse folding models tend to fall into "safe" local minima, generating sequences with repetitive motifs (e.g., excessive electrostatic patterns like poly-EK or hydrophobic poly-A stretches) that optimize theoretical likelihood but fail restricted biophysical binding constraints for difficult targets. In contrast, co-design learns to exploit more complex sequence patterns that are still compatible with the structural constraints of the backbone, allowing the model to navigate out of the structural bottlenecks that trap fixed-backbone sequence designers.

**Decoding Mechanisms** We further compare the co-design mechanisms of SeedProteo with diffusion-based baselines, including RFDiffusion3 and BoltzGen, while excluding PXDdesign and RFDiffusion as they are limited to backbone design rather than all-atom modeling. Both RFDiffusion3 and BoltzGen utilize variants of the atom14 schema, relying on removing specific virtual atoms to implicitly decode amino acid types. In contrast, SeedProteo employs atom14 strictly as a geometric input representation, while the final sequence identity is inferred via a Markov Random Field (MRF) module. This allows our model to capture higher-order residue dependencies that simple geometric decoding might miss.

### 3.4 Ablation Study

**Impact of Secondary Structure Constraints** To evaluate the specific contribution of secondary structure (SS) constraints, we compare our approach against a baseline termed **SeedProteo-M**, which performs binder design using fully masked SS sequences as condition. As shown in Table 3, incorporating secondary structure (SS) sequences as conditioning constraints significantly enhances design success. This constraint effectively prunes the search space, guiding the diffusion process toward *de novo*-like fold topologies.

**Impact of MRF module** To validate the effectiveness of our sequence decoding module, we conducted a supplementary ablation study on unconditional generation (Table 4). We established a baseline that predicts amino acid identities by aggregating features from the atom14 representation at each residue position, a strategy adopted by the recent method [13].

As shown in Table 4, while the baseline achieves competitive performance on short sequences (Length 100), its capability degrades significantly as protein size increases. We reason this divergence to the inherent limitations of the decoding receptive fields. The atom14 schema relies on recognizing amino acid types via local side-chain geometry (implicit conformational recognition). However, the underlying AF3-based architecture primarily models pairwise inductive biases and may lack the capacity to capture long-range atomic dependencies solely through local atoms aggregation. Consequently, the baseline struggles to maintain global consistency in larger systems. Conversely, the MRF module explicitly leverages global pairwise features during inference. By modeling the sequence distribution conditional on the entire backbone topology, the MRF ensures that the

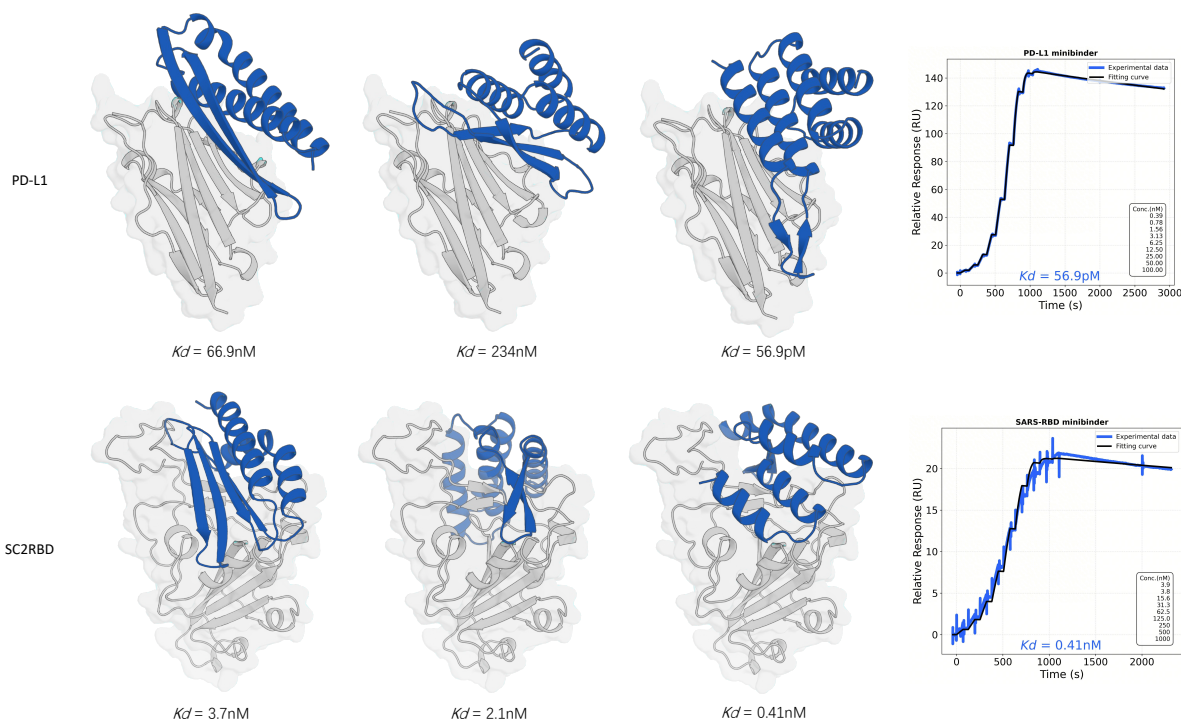


**Figure 4** Wet-lab validation of SeedProteo-designed binders. For each target (PD-L1, top; SC2RBD, bottom), three representative binding complex structures are shown alongside the SPR sensorgram of the highest-affinity binder.

generated sequence is self-consistent with long-range structural constraints, thereby preventing the structural degeneration observed in the baseline at longer lengths.

## 4 In Vitro Experiments

To validate the practical utility of SeedProteo beyond in-silico metrics, we conducted wet-lab experiments on two therapeutically relevant protein targets: the SARS-CoV-2 receptor-binding domain (SC2RBD) [34] and Programmed Death-Ligand 1 (PD-L1) [35]. These targets were selected due to their high clinical relevance—SC2RBD is a primary target for COVID-19 therapeutic antibody development, while PD-L1 is a critical immune checkpoint widely pursued in cancer immunotherapy—as well as their structural diversity, which allows us to assess the generalizability of our model across distinct binding interfaces.

For each target, we generated several thousand minibinders using SeedProteo. The structures passing the in-silico criteria were further clustered using Foldseek to ensure structural diversity, from which 10 representative minibinders were selected per target for experimental characterization. The selected minibinders were recombinantly expressed in *E. coli* with an N-terminal His-SUMO tag and purified via Ni-NTA affinity chromatography followed by size-exclusion chromatography (detailed protocols in Appendix D.1). Binding properties were characterized using surface plasmon resonance (SPR) on a Biacore 8K+ instrument, where candidates were first screened at two concentrations and then subjected to kinetic affinity measurements using either single-cycle or multi-cycle protocols (Appendix D.2). Protein expression and SPR assays for all designed candidates were performed by WuXi AppTec (China).

As shown in Figure 4, SeedProteo achieved hit rates of 70%–80% across both targets, with the best binders reaching picomolar affinity for PD-L1 and sub-nanomolar affinity for SC2RBD. These results demonstrate that our in-silico design pipeline reliably produces binders with strong experimental binding, bridging the gap between computational prediction and wet-lab validation.

## 5 Conclusion

In this work, we presented SeedProteo, a diffusion-based all-atom protein design model. Our empirical benchmarks demonstrate that SeedProteo exhibits superior robustness across long sequences and complex topologies in unconditional design. Furthermore, it achieves state-of-the-art performance among open-source methods for binder design, particularly on hard and multi-chain targets. While effective co-design remains an open challenge in the field, we offer specific insights into achieving superior sequence-structure consistency via a global MRF module. Crucially, our wet-lab validation demonstrates that these in-silico advantages carry over to real-world efficacy, yielding experimentally confirmed binders with high hit rates and picomolar-level affinities. We hope these findings will inspire significant community efforts to further advance the frontier of simultaneous sequence-structure generation.

## **6 Revision History**

### **Version 2, February 24, 2026**

- Added in vitro experimental validation results.
  - Added wet-lab experiments results with SPR binding characterization on SC2RBD and PD-L1 targets.
  - Added revision history section.
- Updated several citations.

### **Version 1, December 31, 2025**

Initial manuscript release.

## Contributions

### Project Lead

Wei Qu<sup>1</sup>

### Contributors

Yiming Ma<sup>1,2,†</sup>, Fei Ye<sup>1</sup>, Chan Lu<sup>1</sup>, Yi Zhou<sup>1</sup>, Kexin Zhang<sup>1,3,†</sup>, Lan Wang<sup>1</sup>, Minrui Gui<sup>1,4,†</sup>

<sup>†</sup> Work is done during their internship at Bytedance Seed.

### Overall Technical Lead

Quanquan Gu<sup>1</sup>

### Affiliation

<sup>1</sup> ByteDance Seed

<sup>2</sup> Peking University

<sup>3</sup> ShanghaiTech University

<sup>4</sup> University of California, Los Angeles

## Acknowledgments

We thank Liang Hong, Zaixiang Zheng, Xinyou Wang, Jiasheng Ye, Jing Yuan, Yilai Li, Zhenghua Wang, Yuning Shen, Cheng-Yen Hsieh, Huizhuo Yuan, as well as other colleagues at ByteDance for their discussions and support.

## References

- [1] J. Dauparas, I. Anishchenko, N. Bennett, H. Bai, R. J. Ragotte, L. F. Milles, B. I. M. Wicky, A. Courbet, R. J. De Haas, N. Bethel, P. J. Y. Leung, T. F. Huddy, S. Pellock, D. Tischer, F. Chan, B. Koepnick, H. Nguyen, A. Kang, B. Sankaran, A. K. Bera, N. P. King, and D. Baker. Robust deep learning-based protein sequence design using ProteinMPNN. *Science*, 378(6615):49–56, October 2022.
- [2] Zaixiang Zheng, Yifan Deng, Dongyu Xue, Yi Zhou, Fei Ye, and Quanquan Gu. Structure-informed Language Models Are Protein Designers. In *Proceedings of the 40th International Conference on Machine Learning*, pages 42317–42338. PMLR, July 2023.
- [3] Sarah Alamdari, Nitya Thakkar, Rianne van den Berg, Neil Tenenholtz, Robert Strome, Alan M. Moses, Alex Lu, Nicolo Fusi, Ava P. Amini, and Kevin Kaichuang Yang. Protein generation with evolutionary diffusion: Sequence is all you need. *bioRxiv : the preprint server for biology*, November 2024.
- [4] Xinyou Wang, Zaixiang Zheng, Fei Ye, Dongyu Xue, Shujian Huang, and Quanquan Gu. Diffusion language models are versatile protein learners. In *International Conference on Machine Learning*, 2024.
- [5] Jason Yim, Brian L. Trippe, Valentin De Bortoli, Emile Mathieu, Arnaud Doucet, Regina Barzilay, and Tommi Jaakkola. SE(3) diffusion model with application to protein backbone generation. In *Proceedings of the 40th International Conference on Machine Learning*, pages 40001–40039. PMLR, July 2023.
- [6] Joseph L. Watson, David Juergens, Nathaniel R. Bennett, Brian L. Trippe, Jason Yim, Helen E. Eisenach, Woody Ahern, Andrew J. Borst, Robert J. Ragotte, Lukas F. Milles, Basile I. M. Wicky, Nikita Hanikel, Samuel J. Pellock, Alexis Courbet, William Sheffler, Jue Wang, Preetham Venkatesh, Isaac Sappington, Susana Vázquez Torres, Anna Lauko, Valentin De Bortoli, Emile Mathieu, Sergey Ovchinnikov, Regina Barzilay, Tommi S. Jaakkola, Frank DiMaio, Minkyung Baek, and David Baker. De novo design of protein structure and function with RFdiffusion. *Nature*, 620(7976):1089–1100, August 2023.
- [7] John B. Ingraham, Max Baranov, Zak Costello, Karl W. Barber, Wujie Wang, Ahmed Ismail, Vincent Frappier, Dana M. Lord, Christopher Ng-Thow-Hing, Erik R. Van Vlack, Shan Tie, Vincent Xue, Sarah C. Cowles, Alan Leung, João V. Rodrigues, Claudio L. Morales-Perez, Alex M. Ayoub, Robin Green, Katherine Puentes, Frank Oplinger, Nishant V. Panwar, Fritz Obermeyer, Adam R. Root, Andrew L. Beam, Frank J. Poelwijk, and Gevorg Grigoryan. Illuminating protein space with a programmable generative model. *Nature*, 623(7989):1070–1078, November 2023.
- [8] Odin Zhang, Xujun Zhang, Haitao Lin, Cheng Tan, Qinghan Wang, Yuanle Mo, Qiantai Feng, Gang Du, Yuntao Yu, Zichang Jin, et al. ODesign: A World Model for Biomolecular Interaction Design. *arXiv preprint arXiv:2510.22304*, 2025.
- [9] Xinyou Wang, Zaixiang Zheng, Fei Ye, Dongyu Xue, Shujian Huang, and Quanquan Gu. Dplm-2: A multimodal diffusion protein language model. In *International Conference on Learning Representations*, 2025.
- [10] Cheng-Yen Hsieh, Xinyou Wang, Daiheng Zhang, Dongyu Xue, Fei Ye, Shujian Huang, Zaixiang Zheng, and Quanquan Gu. Elucidating the design space of multimodal protein language models. In *International Conference on Machine Learning*, 2025.
- [11] Ruizhe Chen, Dongyu Xue, Xiangxin Zhou, Zaixiang Zheng, Xiangxiang Zeng, and Quanquan Gu. An all-atom generative model for designing protein complexes. In *International Conference on Machine Learning*, 2025.
- [12] Andrew Campbell, Jason Yim, Regina Barzilay, Tom Rainforth, and Tommi Jaakkola. Generative flows on discrete state-spaces: Enabling multimodal flows with applications to protein co-design. *arXiv preprint arXiv:2402.04997*, 2024.
- [13] Wei Qu, Jiawei Guan, Rui Ma, kezhai, Weikun.Wu, and Haobo Wang. P(all-atom) Is Unlocking New Path For Protein Design. In *Forty-Second International Conference on Machine Learning*, June 2025.
- [14] Tomas Geffner, Kieran Didi, Zhonglin Cao, Danny Reidenbach, Zuobai Zhang, Christian Dallago, Emine Kucukbenli, Karsten Kreis, and Arash Vahdat. La-Proteina: Atomistic Protein Generation via Partially Latent Flow Matching, July 2025.
- [15] Vinicius Zambaldi, David La, Alexander E Chu, Harshnira Patani, Amy E Danson, Tristan OC Kwan, Thomas Frerix, Rosalia G Schneider, David Saxton, Ashok Thillaisundaram, et al. De novo design of high-affinity protein binders with AlphaProteo. *arXiv preprint arXiv:2409.08022*, 2024.

- [16] Martin Pacesa, Lennart Nickel, Christian Schellhaas, Joseph Schmidt, Ekaterina Pyatova, Lucas Kissling, Patrick Barendse, Jagrity Choudhury, Srajan Kapoor, Ana Alcaraz-Serna, Yehlin Cho, Kourosh H. Ghamary, Laura Vinué, Brahm J. Yachnin, Andrew M. Wollacott, Stephen Buckley, Adrie H. Westphal, Simon Lindhoud, Sandrine Georgeon, Casper A. Goverde, Georgios N. Hatzopoulos, Pierre Gönczy, Yannick D. Muller, Gerald Schwank, Daan C. Swarts, Alex J. Vecchio, Bernard L. Schneider, Sergey Ovchinnikov, and Bruno E. Correia. One-shot design of functional protein binders with BindCraft. *Nature*, August 2025.
- [17] Milong Ren, Jinyuan Sun, Jiaqi Guan, Cong Liu, Chengyue Gong, Yuzhe Wang, Lan Wang, Qixu Cai, Xinshi Chen, Wenzhi Xiao, et al. Pxdesign: Fast, modular, and accurate de novo design of protein binders. *bioRxiv*, pages 2025–08, 2025.
- [18] Jasper Butcher, Rohith Krishna, Raktim Mitra, Rafael I Brent, Yanjing Li, Nathaniel Corley, Paul T Kim, Jonathan Funk, Simon Mathis, Saman Salike, et al. De novo design of all-atom biomolecular interactions with rfdiffusion3. *bioRxiv*, pages 2025–09, 2025.
- [19] Chai Discovery Team, Jacques Boitreaud, Jack Dent, Danny Geisz, Matthew McPartlon, Joshua Meier, Zhuoran Qiao, Alex Rogozhnikov, Nathan Rollins, Paul Wollenhaupt, et al. Zero-shot antibody design in a 24-well plate. *bioRxiv*, pages 2025–07, 2025.
- [20] Latent Labs Team, Alex Bridgland, Jonathan Crabbé, Henry Kenlay, Daniella Pretorius, Sebastian M Schmon, Agrin Hilmkil, Rebecca Bartke-Croughan, Robin Rombach, Michael Flashman, et al. Latent-X: An Atom-level Frontier Model for De Novo Protein Binder Design. *arXiv preprint arXiv:2507.19375*, 2025.
- [21] Josh Abramson, Jonas Adler, Jack Dunger, Richard Evans, Tim Green, Alexander Pritzel, Olaf Ronneberger, Lindsay Willmore, Andrew J. Ballard, Joshua Bambrick, Sebastian W. Bodenstein, David A. Evans, Chia-Chun Hung, Michael O’Neill, David Reiman, Kathryn Tunyasuvunakool, Zachary Wu, Akvilė Žemgulytė, Eirini Arvaniti, Charles Beattie, Ottavia Bertolli, Alex Bridgland, Alexey Cherepanov, Miles Congreve, Alexander I. Cowen-Rivers, Andrew Cowie, Michael Figurnov, Fabian B. Fuchs, Hannah Gladman, Rishub Jain, Yousuf A. Khan, Caroline M. R. Low, Kuba Perlin, Anna Potapenko, Pascal Savy, Sukhdeep Singh, Adrian Stecula, Ashok Thillaisundaram, Catherine Tong, Sergei Yakneen, Ellen D. Zhong, Michal Zielinski, Augustin Židek, Victor Bapst, Pushmeet Kohli, Max Jaderberg, Demis Hassabis, and John M. Jumper. Accurate structure prediction of biomolecular interactions with AlphaFold 3. *Nature*, May 2024.
- [22] Jeremy Wohlwend, Gabriele Corso, Saro Passaro, Noah Getz, Mateo Reveiz, Ken Leidal, Wojtek Swiderski, Liam Atkinson, Tally Portnoi, Itamar Chinn, Jacob Silterra, Tommi Jaakkola, and Regina Barzilay. Boltz-1: Democratizing Biomolecular Interaction Modeling, November 2024.
- [23] Saro Passaro, Gabriele Corso, Jeremy Wohlwend, Mateo Reveiz, Stephan Thaler, Vignesh Ram Somnath, Noah Getz, Tally Portnoi, Julien Roy, Hannes Stark, David Kwabi-Addo, Dominique Beaini, Tommi Jaakkola, and Regina Barzilay. Towards Accurate and Efficient Binding Affinity Prediction.
- [24] Ting Chen, Ruixiang Zhang, and Geoffrey Hinton. Analog bits: Generating discrete data using diffusion models with self-conditioning. *arXiv preprint arXiv:2208.04202*, 2022.
- [25] Donald Metzler and W Bruce Croft. A markov random field model for term dependencies. In *Proceedings of the 28th annual international ACM SIGIR conference on Research and development in information retrieval*, pages 472–479, 2005.
- [26] Hannes Stark, Felix Faltings, MinGyu Choi, Yuxin Xie, Eunsu Hur, Timothy O’Donnell, Anton Bushuiev, Talip Uçar, Saro Passaro, Weian Mao, Mateo Reveiz, Roman Bushuiev, Tomáš Pluskal, Josef Sivic, Karsten Kreis, Arash Vahdat, Shamayeeta Ray, Jonathan T Goldstein, Andrew Savinov, Jacob A Hambalek, Anshika Gupta, Diego A Taquiri-Diaz, Yaotian Zhang, A Katherine Hatstat, Angelika Arada, Nam Hyeong Kim, Ethel Tackie-Yarboi, Dylan Boselli, Lee Schnaider, Chang C Liu, Gene-Wei Li, Denes Hnisz, David M Sabatini, William F DeGrado, Jeremy Wohlwend, Gabriele Corso, Regina Barzilay, and Tommi Jaakkola. Toward Universal Binder Design.
- [27] Milong Ren, Chungong Yu, Dongbo Bu, and Haicang Zhang. Accurate and robust protein sequence design with CarbonDesign. *Nature Machine Intelligence*, 6(5):536–547, May 2024.
- [28] Barthelemy Meynard-Piganeau, Carlo Lucibello, Christoph Feinauer, et al. Fast Uncovering of Protein Sequence Diversity from Structure. In *The Thirteenth International Conference on Learning Representations*.
- [29] Sivaraman Balakrishnan, Hetunandan Kamisetty, Jaime G. Carbonell, Su-In Lee, and Christopher James Langmead. Learning generative models for protein fold families. *Proteins: Structure, Function, and Bioinformatics*, 79(4):1061–1078, April 2011.

- [30] Maarten L Hekkelman, Daniel Álvarez Salmoral, Anastassis Perrakis, and Robbie P Joosten. DSSP 4: FAIR annotation of protein secondary structure. *Protein Science*, 34(8):e70208, 2025.
- [31] Tomas Geffner, Kieran Didi, Zuobai Zhang, Danny Reidenbach, Zhonglin Cao, Jason Yim, Mario Geiger, Christian Dallago, Emine Kucukbenli, Arash Vahdat, and Karsten Kreis. Proteina: Scaling Flow-based Protein Structure Generative Models. In *The Thirteenth International Conference on Learning Representations*, October 2024.
- [32] Ivan Anishchenko, Samuel J. Pellock, Tamuka M. Chidyausiku, Theresa A. Ramelot, Sergey Ovchinnikov, Jingzhou Hao, Khushboo Bafna, Christoffer Norn, Alex Kang, Asim K. Bera, Frank DiMaio, Lauren Carter, Cameron M. Chow, Gaetano T. Montelione, and David Baker. De Novo Protein Design by Deep Network Hallucination. *Nature*, 600(7889):547–552, December 2021.
- [33] Yi Zhou, Chan Lu, Yiming Ma, Wei Qu, Fei Ye, Kexin Zhang, Lan Wang, Minrui Gui, and Quanquan Gu. SeedFold: Scaling Biomolecular Structure Prediction. *arXiv preprint*, 2025.
- [34] Longxing Cao, Inna Goreschnik, Brian Coventry, James Brett Case, Lauren Miller, Lisa Kozodoy, Rita E Chen, Lauren Carter, Alexandra C Walls, Young-Jun Park, et al. De novo design of picomolar SARS-CoV-2 miniprotein inhibitors. *Science*, 370(6515):426–431, 2020.
- [35] Wei Yang, Derrick R Hicks, Agnidipta Ghosh, Tristin A Schwartz, Brian Coventry, Inna Goreschnik, Aza Allen, Samer F Halabiya, Chan John Kim, Cynthia S Hinck, et al. Design of high-affinity binders to immune modulating receptors for cancer immunotherapy. *Nature communications*, 16(1):2001, 2025.
- [36] Mihaly Varadi, Stephen Anyango, Mandar Deshpande, Sreenath Nair, Cindy Natassia, Galabina Yordanova, David Yuan, Oana Stroe, Gemma Wood, Agata Laydon, Augustin Židek, Tim Green, Kathryn Tunyasuvunakool, Stig Petersen, John Jumper, Ellen Clancy, Richard Green, Ankur Vora, Mira Lutfi, Michael Figurnov, Andrew Cowie, Nicole Hobbs, Pushmeet Kohli, Gerard Kleywegt, Ewan Birney, Demis Hassabis, and Sameer Velankar. AlphaFold Protein Structure Database: Massively expanding the structural coverage of protein-sequence space with high-accuracy models. *Nucleic Acids Research*, 50(D1):D439–D444, January 2022.
- [37] Zeming Lin, Halil Akin, Roshan Rao, Brian Hie, Zhongkai Zhu, Wenting Lu, Nikita Smetanin, Robert Verkuil, Ori Kabeli, Yaniv Shmueli, et al. Evolutionary-scale prediction of atomic-level protein structure with a language model. *Science*, 379(6637):1123–1130, 2023.
- [38] Helen M Berman, John Westbrook, Zukang Feng, Gary Gilliland, Talapady N Bhat, Helge Weissig, Ilya N Shindyalov, and Philip E Bourne. The protein data bank. *Nucleic acids research*, 28(1):235–242, 2000.
- [39] Daniel Kovtun, Mehmet Akdel, Alexander Goncarencu, Guoqing Zhou, Graham Holt, David Baugher, Dejun Lin, Yusuf Adeshina, Thomas Castiglione, Xiaoyun Wang, et al. PINDER: The protein interaction dataset and evaluation resource. *bioRxiv*, pages 2024–07, 2024.
- [40] Jing Zhang, Ian R. Humphreys, Jimin Pei, Jinuk Kim, Chulwon Choi, Rongqing Yuan, Jesse Durham, Siqi Liu, Hee-Jung Choi, Minkyung Baek, David Baker, and Qian Cong. Predicting Protein-Protein Interactions in the Human Proteome. *Science*, 390(6771):eadt1630, October 2025.
- [41] Lorna Richardson, Ben Allen, Germana Baldi, Martin Beracochea, Maxwell L Bileschi, Tony Burdett, Josephine Burgin, Juan Caballero-Pérez, Guy Cochrane, Lucy J Colwell, et al. MGnify: the microbiome sequence data analysis resource in 2023. *Nucleic acids research*, 51(D1):D753–D759, 2023.
- [42] John Jumper, Richard Evans, Alexander Pritzel, Tim Green, Michael Figurnov, Olaf Ronneberger, Kathryn Tunyasuvunakool, Russ Bates, Augustin Židek, Anna Potapenko, et al. Highly accurate protein structure prediction with AlphaFold. *nature*, 596(7873):583–589, 2021.
- [43] Michel Van Kempen, Stephanie S. Kim, Charlotte Tumescheit, Milot Mirdita, Jeongjae Lee, Cameron L. M. Gilchrist, Johannes Söding, and Martin Steinegger. Fast and accurate protein structure search with Foldseek. *Nature Biotechnology*, 42(2):243–246, February 2024.
- [44] Martin Steinegger and Johannes Söding. MMseqs2 enables sensitive protein sequence searching for the analysis of massive data sets. *Nature Biotechnology*, 35(11):1026–1028, November 2017.
- [45] Andy M Lau, Nicola Bordin, Shaun M Kandathil, Ian Sillitoe, Vaishali P Waman, Jude Wells, Christine A Orenge, and David T Jones. Exploring structural diversity across the protein universe with The Encyclopedia of Domains. *Science*, 386(6721):eadq4946, 2024.

# Appendix

## A Data Preparation and Curation

Training a foundation model for protein design, particularly one capable of binder generation, necessitates a diverse corpus comprising both monomeric and multimeric structures. While predicted monomer databases such as the AlphaFold Database (AFDB) [36] and ESMAtlas [37] provide extensive coverage of single-chain structures, existing multimer datasets derived from the RCSB PDB [38] are limited in scale and often unsuitable for the specific two-chain requirements of binder design tasks. To address this, we constructed a composite training dataset by integrating curated monomer data with multimeric interactions sourced from Pinder [39] and HumanPPI [40]. We detail the processing and filtering pipelines for each category below.

### A.1 Monomer Data Curation

Our monomeric dataset is derived exclusively from AFDB and ESMAtlas. For the ESMAtlas component, to mitigate potential quality issues associated with ESMFold [37] predictions, we retrieved the corresponding sequences from the MGnify database [41] and re-predicted their structures using AlphaFold2 (AF2) [42].

To ensure high data quality, we applied the following inclusion criteria to all monomer structures:

- Sequence length between 50 and 768 residues.
- Average pLDDT score  $> 80$ .
- Secondary structure coil fraction  $< 50\%$ .

To eliminate redundancy, we performed clustering using Foldseek [43] and MMseqs2 [44] and retained only the cluster representatives (centroids). The final curated monomer dataset consists of approximately 0.5 million structures. Sequences that can be folded by SeedFold [33] in a single-sequence setting are exclusively allocated for the training of the initial phase.

### A.2 Multimer Data Curation

Protein-Protein Interactions (PPIs) are fundamental to training a robust binder design model. We sourced multimer data from two primary streams to cover experimentally determined interactions and high-quality predicted domain interactions.

**Experimental PPIs (Pinder).** To align our training data with the standard inference scenario, where a binder chain is designed for a specific target chain, we utilized the Pinder dataset. Using the curated holo-structure PDB IDs and chain IDs provided by Pinder, we extracted relevant substructures from RCSB biological assemblies. We filtered these two-chain complexes by requiring: (1) a coil fraction of  $< 50\%$  for each chain, and (2) a minimum interfacial  $C_\beta$  distance of  $< 8\text{\AA}$  to ensure meaningful contact. Following structural clustering via Foldseek-Multimer, we retained approximately 50,000 unique cluster representatives.

**Augmented DDI Dataset (HumanPPI).** To overcome the scarcity of experimental PPI data, we augmented our training set with domain-domain interactions (DDIs). This approach relies on the established hypothesis that intrachain DDI interfaces resemble interchain PPI interfaces in terms of coevolutionary and physicochemical properties [45]. We utilized the HumanPPI database, which distills DDIs from accurately predicted monomer structures in the AFDB. We applied the identical filtering and clustering pipeline used for the Pinder dataset (coil check and distance constraints). This augmentation yielded an additional  $\sim 0.1$  million interaction pairs.

## B Evaluation Settings

**Table 5 Training Stages.**

Hyperparameter	Stage 1 (Initial)	Stage 2 (Fine-tuning 1)	Stage 3 (Fine-tuning 2)
Crop Size	384	768	768
Batch Size	128	64	64
Motif Percentage	0%	20%	20%
Training Steps	50K	20K	30K
<i>Data Sampling Distribution</i>			
Strictly Filtered Monomer	100%	20%	10%
Expanded Monomer Data	–	80%	40%
Multimer Data	–	–	50%

## B.1 Unconditional Generation Evaluation

For unconditional monomer generation, we employ a self-consistency assessment pipeline to evaluate structural designability. For each generated backbone, we first only derive **one** amino acid sequence using ProteinMPNN (inverse folding). The sequence is subsequently refolded using SeedFold, an AlphaFold3-like folding model in a single-sequence setting. A design is considered successful if it satisfies two criteria: (1) the  $C\alpha$ -RMSD between the generated backbone and the refolded structure is  $< 2.0\text{\AA}$ , and (2) the average pLDDT score of the refolded structure is  $> 80$ . Metrics for **structural diversity** (number of unique structural clusters) and **novelty** (maximum TM-score relative to the PDB) are calculated with Foldseek [43] exclusively on the subset of designable cases.

**Topology-Aware Analysis.** To address the long-standing challenge in protein generative models, specifically the bias toward  $\alpha$ -helical structures and the difficulty in generating valid  $\beta$ -sheets, we incorporate a fine-grained analysis based on secondary structure topology. Based on secondary structure proportions, we classify the generated proteins into three distinct fold types. We define **EEE** (primarily  $\beta$ -sheet) as structures with over 40% sheet and under 20% helix content, and **HHH** (primarily  $\alpha$ -helical) as those with over 50% helix and under 10% sheet content; both categories require a loop fraction below 45%. All remaining structures are categorized as hybrid Helix-E-Loop (**HEL**).

## B.2 Binder Design Evaluation

We evaluate binder design performance on a benchmark set of 10 targets, consistent with the validation set used in AlphaProteo (see Table 6). To rigorously assess the upper bound of design capability across different length scales, we adopt a dense sampling strategy: for each target, we sample 100 candidates at every 5-residue interval within the target-specific binder length range. For example, for the SC2RBD target (length range 80–120 residues), this results in a total of 900 sampled candidates.

For sequence recovery, we generate two sequences for each designed binder backbone using SolubleMPNN at a sampling temperature of  $\tau = 0.001$ . The designs are then validated using SeedFold in single sequence with target template mode. A binder design is considered successful if it meets the following criteria:

- Interface Predicted Aligned Error (min PAE interaction)  $< 1.5$ ;
- Binder pTM score  $> 0.8$ ;
- Complex RMSD  $< 2.5\text{\AA}$ .

## C Baseline Sampling

In this section, we detail the specific configurations, checkpoints, and codebases used for all baseline methods included in our benchmarks.

**Table 6 Benchmark Dataset for Binder Design.** We evaluated performance on 10 diverse targets. The table lists the target details, including the PDB ID, the specific chains/residues used as the target region, the key hotspot residues defining the binding site, and the range of binder lengths sampled during inference.

Target	PDB ID	Target Region	Hotspot Residues	Length Range
<b>BHRF1</b>	2wh6	Chain A: 2-158	A65, A74, A77, A82, A85, A93	80-120
<b>SC2RBD</b>	6m0j	Chain E: 333-526	E485, E489, E494, E500, E505	80-120
<b>IL-7RA</b>	3di3	Chain B: 17-209	B58, B80, B139	50-120
<b>PD-L1</b>	5o45	Chain A: 17-132	A56, A115, A123	50-120
<b>TrkA</b>	1www	Chain X: 282-382	X294, X296, X333	50-120
<b>Insulin</b>	4zxb	Chain E: 6-155	E64, E88, E96	40-120
<b>H1</b>	5v1i	Chain A: 1-50, 76-80, 107-111, 258-322; Chain B: 1-68, 80-170	B21, B45, B52	40-120
<b>VEGF-A</b>	1bj1	Chain V: 14-107; Chain W: 14-107	W81, W83, W91	50-140
<b>IL-17A</b>	4hsa	Chain A: 17-131; Chain B: 19-127	A94, A116, B67	50-140
<b>TNF<math>\alpha</math></b>	1tnf	Chain A/B/C: 12-157	A113, C73	50-120

## C.1 Unconditional Benchmark

**La-Proteina.** We utilized the official implementation and checkpoints provided in the La-Proteina repository<sup>1</sup>. To ensure optimal performance across different scales, we selected checkpoints based on the target sequence length: the LD1\_ucond\_notri\_512.ckpt checkpoint was used for lengths 100–500, while LD3\_ucond\_notri\_800.ckpt was employed for lengths 600–1000. All sampling was conducted using the default inference configurations.

**Proteina.** We used the code and checkpoints from the official Proteina repository<sup>2</sup>. Similar to La-Proteina, we adopted a length-dependent checkpoint strategy: proteina\_v1.1\_DFS\_200M\_tir.ckpt was used for lengths 100–500, and proteina\_v1.6\_DFS\_200M\_notri\_long\_chain\_generation.ckpt was used for lengths 600–1000. Default sampling parameters were applied in all cases.

**RFDiffusion.** We employed the official codebase available at the RFDiffusion repository<sup>3</sup>. All unconditional generation tasks were performed using the standard default sampling configurations provided by the authors.

## C.2 Binder Design Benchmark

For the binder design task, all methods utilize identical target structures (in mmCIF format) and are conditioned on the exact same set of hotspot residues. For each target, we generate an equal number of candidate proteins with consistent lengths across all models. To ensure a fair comparison of generative capabilities, we disable any built-in auxiliary modules—such as pre-filtering, ranking, or early-stopping strategies—thereby restricting the evaluation strictly to the core sampling function.

**BindCraft.** We utilized the official implementation from the BindCraft repository<sup>4</sup>. For binder generation, we adopted the default\_4stage\_multimer configuration under the advanced setting. To ensure a fair evaluation of the generative capability without post-hoc selection bias, we disabled both the filtering stage and the early stopping strategy. This ensured that every sampling attempt was completed and all raw outputs were retained, regardless of their internal quality metrics.

**BoltzGen.** We performed evaluations using the code provided in the BoltzGen repository<sup>5</sup>, specifically utilizing commit SHA 58c1eed. We employed the protein-anything protocol for inference. To bypass internal ranking and filtering mechanisms, we set the inference budget equal to the number of desired designs, ensuring a direct one-to-one output.

<sup>1</sup><https://github.com/NVIDIA-Digital-Bio/la-proteina>

<sup>2</sup><https://github.com/NVIDIA-Digital-Bio/proteina>

<sup>3</sup><https://github.com/RosettaCommons/Rfdiffusion>

<sup>4</sup><https://github.com/martinpacesa/BindCraft>

<sup>5</sup><https://github.com/HannesStark/boltzgen>

**RFDiffusion.** For binder design tasks, we set both `noise_scale_ca` and `noise_scale_frame` to 0 during sampling. The authors suggest that this deterministic setting yields superior performance for specific binder design scenarios.

**RFDiffusion3.** We utilized the implementation available in the RosettaCommons Foundry repository<sup>6</sup>, specifically commit SHA 7f6656e. We set `align_trajectory_structures=False` to prevent potential runtime errors during trajectory processing; all other configurations were maintained at default values.

**PXDesign.** We utilized the implementation in the PXDesign repository<sup>7</sup>, specifically commit SHA ec6615c. We perform binder design for each target of a given hotspot using `Generation Only` mode.

## D In Vitro Experimental Protocols

### D.1 Protein Production

**PD-L1.** The extracellular domain of PD-L1 (residues 18–239) was cloned into pcDNA3.1 and expressed as a secreted protein in Expi293F cells via transient transfection with polyethylenimine (PEI). Transfection was performed when suspension cultures grown at 37 °C reached a density of  $3 \times 10^6$  cells/mL. Sodium butyrate (10 mM) was supplemented 9 hours post-transfection to enhance expression. Culture supernatants were harvested 5 days post-transfection. The pH was adjusted by adding 20 mM bis-tris propane (BTP) before loading onto Ni Sepharose Excel resin. The resin was washed with 10 column volumes of wash buffer (20 mM Na<sub>2</sub>HPO<sub>4</sub>/NaH<sub>2</sub>PO<sub>4</sub>, 200 mM NaCl, 20 mM imidazole, pH 7.4) and eluted with elution buffer (20 mM Na<sub>2</sub>HPO<sub>4</sub>/NaH<sub>2</sub>PO<sub>4</sub>, 200 mM NaCl, 300 mM imidazole, pH 7.4). The eluate was dialyzed and incubated with TEV protease for tag cleavage. The digested sample was passed over a Ni resin column; the flow-through was collected, concentrated, and further purified by gel-filtration chromatography on a Superdex 75 column equilibrated with SEC buffer (10 mM Na<sub>2</sub>HPO<sub>4</sub>, 1.8 mM KH<sub>2</sub>PO<sub>4</sub>, 137 mM NaCl, 2.7 mM KCl, pH 7.4). Peak fractions were pooled and concentrated to the desired concentration for downstream assays.

**SARS-CoV-2 RBD.** The SARS-CoV-2 receptor-binding domain (SC2RBD) was obtained commercially from AcroBiosystems (Cat. # SPD-C82E9).

**Minibinder Expression and Purification.** Minibinder sequences were cloned with an N-terminal His-SUMO tag into a custom expression vector and transformed into BL21-CodonPlus (DE3)-RIPL *E. coli*. Cultures were grown in Terrific Broth at 37 °C until OD<sub>600</sub> reached 0.75, then induced with 1 mM isopropyl- $\beta$ -D-thiogalactopyranoside (IPTG) for 4 hours at 37 °C. Cells were lysed by high-pressure homogenization in lysis buffer (50 mM HEPES pH 8.0, 100 mM NaCl, 1 mM TCEP, 1 mM EDTA, supplemented with cOmplete EDTA-free protease inhibitor at 1 tablet per 100 mL). Proteins were purified by Ni-NTA chromatography, with the column washed using lysis buffer supplemented with 30 mM imidazole and eluted with 250 mM imidazole. The eluate was subjected to size-exclusion chromatography on a Superdex 200 10/300 GL column in 50 mM HEPES pH 8.0, 100 mM NaCl, 1 mM TCEP, 1 mM EDTA. Peak fractions were collected and stored for subsequent binding assays.

### D.2 Surface Plasmon Resonance (SPR)

SPR experiments were performed on a Biacore 8K+ instrument (GE Healthcare) at 25 °C. Target proteins were immobilized on a Series S Sensor Chip SA (streptavidin, GE Healthcare) via biotin capture. The assay buffer consisted of 50 mM HEPES, 100 mM NaCl, 1 mM TCEP, and 1 mM EDTA at pH 8.0. The chip surface was activated with 1 M NaCl/50 mM NaOH (contact time: 60 s, flow rate: 30  $\mu$ L/min), after which the biotinylated target protein was prepared at 1  $\mu$ g/mL in assay buffer and coupled to the streptavidin surface to a density of approximately 100 Response Units (RU).

Minibinder stock solutions were maintained in the same assay buffer. For primary screening, each minibinder was tested at 10 $\times$  and 50 $\times$  dilutions of the stock concentration, along with a zero-concentration reference for

<sup>6</sup><https://github.com/RosettaCommons/foundry>

<sup>7</sup><https://github.com/bytedance/PXDesign>

background subtraction. Candidates were selected for affinity testing based on curve shape and RU response.

For affinity determination, either single-cycle kinetics (contact time: 70 s, dissociation time: 1200 s, flow rate: 30  $\mu\text{L}/\text{min}$ , 9-point 1:1 serial dilution) or multi-cycle kinetics (contact time: 70 s, dissociation time: 600 s, flow rate: 30  $\mu\text{L}/\text{min}$ , 12-point 1:1 serial dilution) were employed based on the estimated affinity of each minibinder. Data were analyzed using Biacore Insight Evaluation Software (version 6.0.7.1750). Kinetic parameters were determined by fitting sensorgrams to the Langmuir 1:1 binding model, which assumes a single-site interaction between the analyte and the immobilized ligand.